www.czasopisma.pan.pl PAN POLSKA AKADEMIA NAUK www.journals.pan.pl

Arch. Metall. Mater. **64** (2019), 1, 167-173

DOI: 10.24425/amm.2019.126233

W. BARTOSZEK*#, M. TRZASKA*

HYBRID NANOCOMPOSITE LAYERS $Ni/Al_2O_3/C_{GRAPHITE}$ PRODUCED BY ELECTROCRYSTALLIZATION METHOD

The paper presents the results of studies of hybrid composite layers $Ni/Al_2O_3/C_{graphite}$ produced by the electrodeposition method. Three variants of hybrid composite layers were prepared in electrolyte solutions with the same amounts of each dispersion phases which were equal to 0.25; 0.50 and 0.75 g/dm^3. The structure of $Ni/Al_2O_3/C_{graphite}$ layers as well as the Al_2O_3 and graphite powders, which were used as dispersion phases was investigated. The results of morphology and surface topography of produced layers are presented. The modulus of elasticity and microhardness of the material of produced layers were determined by DSI method. Tribological and corrosion resistance tests of produced layers were carried out. Realized studies have shown that the material of the produced layers is characterized by a nanocrystalline structure. Incorporation of dispersion phases into the nickiel matrix increases the degree of surface development of layers. $Ni/Al_2O_3/C_{graphite}$ layers are characterized by high hardness and abrasion resistance by friction, furthermore, they provide good corrosion protection for the substrate material.

Keywords: hybrid composite layers, electrocrystallization, nickel layers, wear resistance, corrosion resistance

1. Introduction

Deposition of metal layers by electrocrystallization method is widely used in industry to improve the useful properties of products, like corrosion or abrasion resistance. Due to increasing requirements for various types of products it is necessary to look for solutions in the form of new materials that would allow to exhibit the best operational parameters in a specific area of application. A high potential to modify the properties of the products is accomplished by applying a layer of a composite material on the given product surface.

Composite layers produced by electrocrystallization method are characterized by much better mechanical and corrosion properties than layers of pure metals, what is confirmed by a number of publications [1-7]. The properties of the produced composite layers can be controlled by appropriate selection of matrix material, type of dispersion phase, size and shape of the dispersion phase particles, proportion and distribution of the dispersion phase incorporated in the matrix material. A new solution of composite layers results from the incorporation of two or more types of dispersion phases with different properties into metal matrix. In such a process a hybrid layer is formed. This type of layers allows to obtain a material that combines many favorable properties. The subject of realized research are hybrid composite layers $Ni/Al_2O_3/C_{graphite}$ with a nanocrystalline structure produced by electrocrystallization method. The combination of three different materials in the composite layer enables mutual complementing of their properties, whereas interactions between them induce the modification of the properties of the whole layer. Due to the content of the dispersion phases used in the composite material and the degree of their dispersion, the desired properties of the produced layer can be achieved.

2. Research methodology

Hybrid composite layers with nickel matrix and Al_2O_3 and graphite as dispersion phases were produced by electrocrystallization method in baths constituting a mixture of multi-component electrolyte and powders of dispersion phases. For comparative purposes, researches include nickel layers produced at the same process parameters. The nanometrical powders of Al_2O_3 and graphite were used as dispersion phases. Three variants of hybrid composite layers were produced in electrolyte solutions containing the same amount of each powder which was equal to 0.25; 0.50 and 0.75 g/dm^3. The chemical composition of baths used to produce the layers is shown in Table 1. Saccharin (4 g/dm^3) and sodium dodecyl sulfate (0.45 g/dm^3) were used as organic compounds to solutions. These substances have an influence on the structure of deposited nickel, resulting into refining of structure to nanometric dimensions [8].

The electrodeposition process was carried out at current density of 3 A/dm^2 in the bath at a temperature of 318 K in ambient atmosphere. During the process of nickel deposition

* DEPARTMENT OF ELECTROPLATING AND ENVIRONMENTAL PROTECTION, INSTITUTE OF PRECISION MECHANICS, 3 DUCHNICKA STR., 01-796 WARSZAWA, POLAND

Corresponding author: wojciech.bartoszek@imp.edu.pl

TABLE 1

Chemical composition of baths

Layer	Chemical composition of baths
Ni	nickel(II) sulfate(VI), boric acid, nickel(II) chloride, organic compounds
$Ni/Al_2O_3/C_{graphite}(0.25)$	nickel(II) sulfate(VI), boric acid, nickel(II) chloride, organic compounds, 0.25 g/dm^3 Al_2O_3, 0.25 g/dm^3 graphite
$Ni/Al_2O_3/C_{graphite}(0.50)$	nickel(II) sulfate(VI), boric acid, nickel(II) chloride, organic compounds, 0.50 g/dm^3 Al_2O_3, 0.50 g/dm^3 graphite
$Ni/Al_2O_3/C_{graphite}(0.75)$	nickel(II) sulfate(VI), boric acid, nickel(II) chloride, organic compounds, 0.75 g/dm^3 Al_2O_3, 0.75 g/dm^3 graphite

hydrogen evolutions were observed. This effect did not cause discontinuities in the volume of the deposited composite material around the particles of the dispersion phases as well as it did not affect the morphology of the surface layers – pittings were not observed. A good dispersion of powders in the bath and avoiding the sedimentation of particles and facilitating their transport during the process were ensured by mechanical stirring with 400 rpm. Layers were deposited on carbon steel 235JR substrate, which was grinded, degreased in $CaCO_3$ and activated in 15% H_2SO_4 before the electrodeposition process. Nickel electrodes were used as the anodes in the electrocrystallization process, which during the process are pulverized, providing nickel ions to the electrolyte. The dispersion phases were characterized by scanning electron microscope JOEL JSM-IT100 LA. In addition, the graphite powder was examined by Raman spectroscope (System inVia Reflex Renishaw) with excitation by laser light of 532 nm wavelength. The surface topography and morphology of produced layers were characterized by scanning electron microscope. The crystalline structure of layers was examined by X-Ray diffraction method using a copper anode lamp with the wavelength $\lambda = 0.154$ nm. To investigate the roughness parameters of surface of the substrate material and produced layers, the tester Surftest SJ 210 was used. The microhardness was examined by the Knoop method at 10 G load (HV0.01) on metallographic cross-sections using the T1202 Wilson-Hardness tester. The DSI tests were carried out using the MHT nanoindentator (CSM Microhardness Tester) with the Vickers indenter, using the maximum indenter load $Fm = 100$ mN, the loading/unloading speed was $V = 200$ mN / min, and the holding time $t = 15$ s. The modulus of elasticity E_{IT}, Indention hardness H_{IT} and Martens hardness H_M were determined by DSI method. Tribological tests were conducted by the ball-on-disc method using the AutoWir-S1 tester. The friction pair was a sample and Ø5 mm diameter grinding ball made of silicon carbide. Measurements of wear resistance were carried out at the ball pressing force equal to 7.35 N. During the test, the sample performed a peripheral motion with a rotational speed of 2 revs/sec, the number of rotations was equal to 100. The corrosion properties of deposited layers and substrate material were tested by potentiodynamic method with the Bio-logic SP-200 system. Measurements were carried out in a three electrode system in 0.5 M NaCl solution at 293 K in ambient atmosphere. As a reference electrode, $Hg/Hg_2Cl_2/KCl$ calomel electrode with a potential +244 mV was used. The platinum electrode was the counter electrode. The tests were conducted in the range of ±250 mV potential versus open circuit potential. Scanning speed was taken as 0.2 mVs^{-1}.

3. Results

To produce hybrid composite layers, a ceramic dispersion phase Al_2O_3 and graphite in forms of polydisperse powders were used. The morphology of particles of Al_2O_3 and graphite powders are shown in Figure 1.

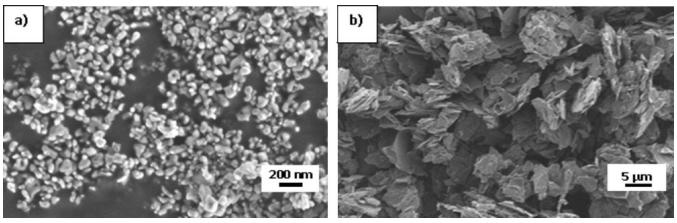

Fig. 1. Image of powder particles of: a) Al_2O_3, b) graphite

The Al_2O_3 powder particles are characterized by irregular shape and nanometric dimensions below 100 nm. The graphite powder particles are characterized by the flake structure and tend to form agglomerates. The sizes of graphite powder particles are below 5 µm.

To characterize the structure of graphite flakes, the Raman spectroscopy was used. Figure 2 shows the Raman spectrum of graphite powder particles.

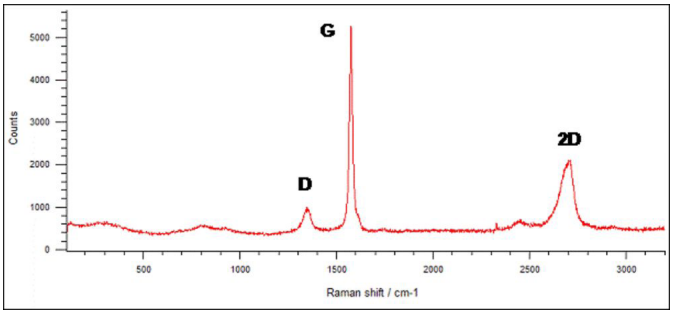

Fig. 2. Raman spectrum of graphite powder

The Raman spectrum is characterized by three peaks, which are characteristic for allotropic carbon varieties with sp^2 hybridization bonds. The first peak D is associated with the structural imperfections of graphite, such as structural defects and the edges of the graphite flakes [9-11]. Broadening of 2D peak informs about the multilayer structure of analyzed graphite powder. The intensity of the G peak is higher than intensity of 2D peak and increases with the increasing of number of graphene layers in the carbon material [12]. A high intensity of G peak

in relation to the 2D ($I_{2D}/I_G < 1$) peak indicates on the graphite structure of the used carbon powder [11, 13]. The results of X-ray diffraction analysis of the nickel and hybrid composite layer structure produced from the bath with the highest content of both dispersion phases are shown in Figure 3.

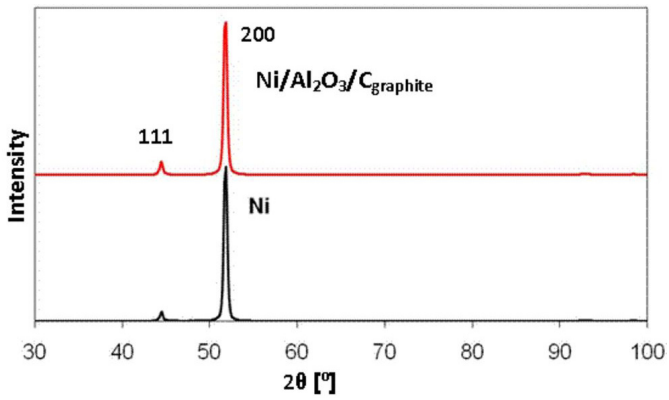

Fig. 3. Diffraction pattern of Ni and $Ni/Al_2O_3/C_{graphite}$ (0.75) layers

Both analyzed materials are characterized by crystalline structure as evidenced by the occurrence of sharp diffraction reflections. In the case of a hybrid composite layer, diffraction reflection of other origin than nickel are not observed. It is the most probably associated with too small amount of powders particles built into the nickel matrix, additionally, the angle range of realized analysis did not include the range of reflection diffraction pattern characteristic for graphite that occurs at an angle of 2θ equal to about 26° [14]. A high intensity of diffraction reflections (200) indicates on the textured structure of produced nickel layers. In order to estimate the size of the crystallites of nickel and hybrid composite layers, the Scherrer formula was used.

$$B = K\lambda/D_{hkl}\cos\theta \qquad (1)$$

where:

B – the peak width of the diffraction peak profile at half maximum height [rad],
K – dimensionless shape factor, adopted $K = 0.9$,
λ – X-Ray wavelenght [nm],
D_{hkl} – average crystallite size [nm],
θ – angle of reflection.

The determined average of crystallites size in the nickel layer was 25 nm, whereas in the hybrid composite layer 22 nm. The structure of layer material has been refining as a result of incorporation of dispersion phases particles into nickel matrix. This is related to the propagation of more nucleation sites by the incorporation of particles of dispersion phases and blocking the growth of crystallites, and the formations of finer crystalline structure of material take places [15-17]. Morphology and surface topography of nickel and hybrid composite layers are shown in Figure 4.

The incorporation of dispersion phases as Al_2O_3 and graphite into nickel matrix increases the degree of surface development of layers. The higher degree of surface development due to built

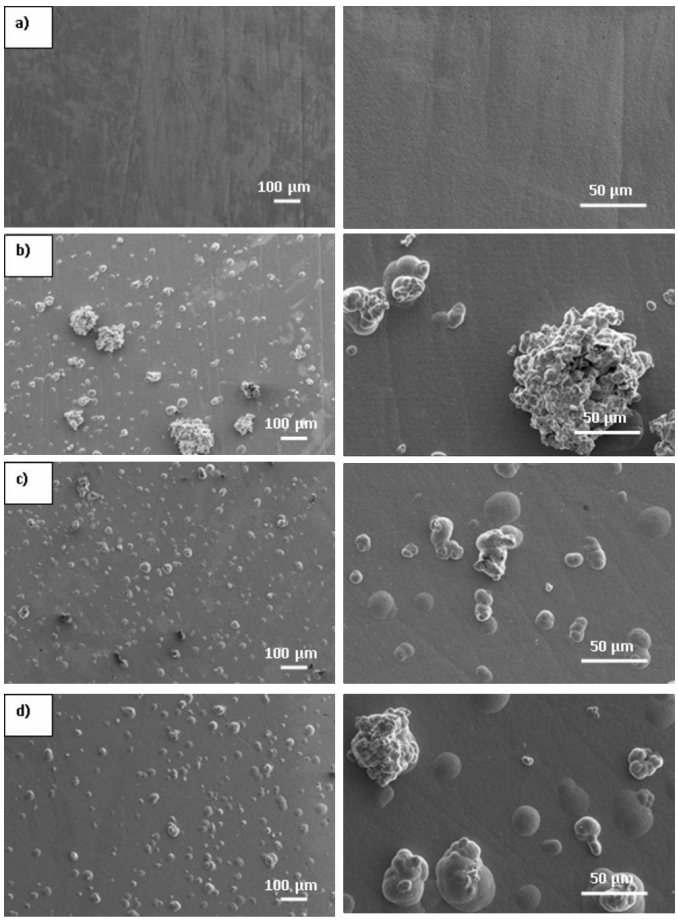

Fig. 4. Morphology and surface topography of the layers: a) Ni, b) $Ni/Al_2O_3/C_{graphite}$ (0.25), c) $Ni/Al_2O_3/C_{graphite}$ (0.50), d) $Ni/Al_2O_3/C_{graphite}$ (0.75)

on and partially over-built graphite particles is observed on the surface of hybrid composite layer produced from the bath with the smallest content of dispersion phases. Whereas the layers produced from the baths with higher content of dispersion phases are characterized by lower degree of surface development in relation to $Ni/Al_2O_3/C_{graphite}$ (0.25). The higher amount of hard ceramic Al_2O_3 phase in the bath during the layer deposition process, in addition to the incorporation, results in the removal of poorly anchored large agglomerates of graphite flakes from the surface as a result of the bath mixing. This prevents the formation of branched forms and leads to reduce the degree of surface development of the deposited layer what correlates with the results of roughness parameters presented in the Table 2. Figure 5 shows the sample cross sections perpendicular to the surface of the layers.

TABLE 2

Roughness parameters of substrate material and deposited layers

Layer	Roughness parameter *Ra* [µm]	
	substrate	layer
Ni	0.071	0.064
$Ni/Al_2O_3/C_{graphite}$ (0.25)	0.061	5.669
$Ni/Al_2O_3/C_{graphite}$ (0.50)	0.102	3.273
$Ni/Al_2O_3/C_{graphite}$ (0.75)	0.093	3.194

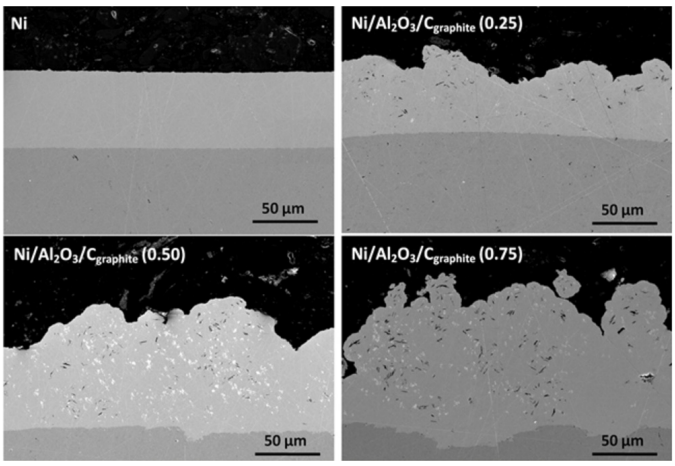

Fig. 5. Cross sections of deposited layers

The produced layers are compact and characterized by good adhesion to the substrate. In the case of hybrid composite layers, the incorporation of graphite particles and Al_2O_3 agglomerates into nickel matrix was identified.

The incorporation of dispersion phases in the forms of graphite flakes and Al_2O_3 powder particles in the volume of produced composite hybrid layers is confirmed by the results of chemical composition analysis using the EDS method what is marked in the areas shown in Figures 6-8 and summarized in Tables 3-5.

It should be emphasized that the presented results of the chemical composition analysis confirm the incorporation of graphite flakes and Al_2O_3 powder particles trough the whole volume of the produced hybrid composite layers.

The results of investigations of corrosion properties of produced layers are presented in Figure 9 in the form of potentiodynamic curves. The corrosion potential and corrosion current density of produced layers were determined on the base of the obtained potentiodynamic curves (Table 6).

Shifting the corrosion potential of hybrid composite layers towards positive values indicates their higher corrosion resistance compared to the nickel layer. The hybrid composite layer produced in the bath with the highest amount of dispersion phases is characterized by the highest corrosion resistance. Several factors have an impact to the improvement of corrosion resistance as a result of incorporation of Al_2O_3 and graphite particles. In the work [18], the higher corrosion resistance of composite layers is explained by the fact that the embedded particles act as physical barriers for the initiation and development of corrosion, furthermore, the dispersion particles limit the area of influences of the corrosion medium on the nickel matrix. Moreover, the refining of crystalline structures of layer

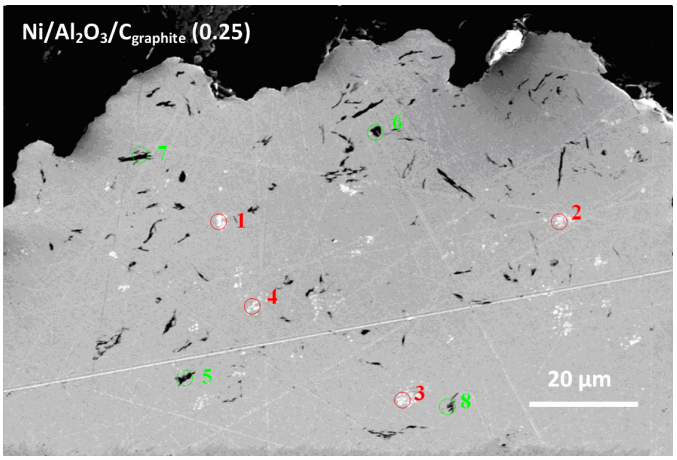

Fig. 6. Cross-section of $Ni/Al_2O_3/C_{graphite}$ (0.25) composite layer with marked areas of chemical composition analysis

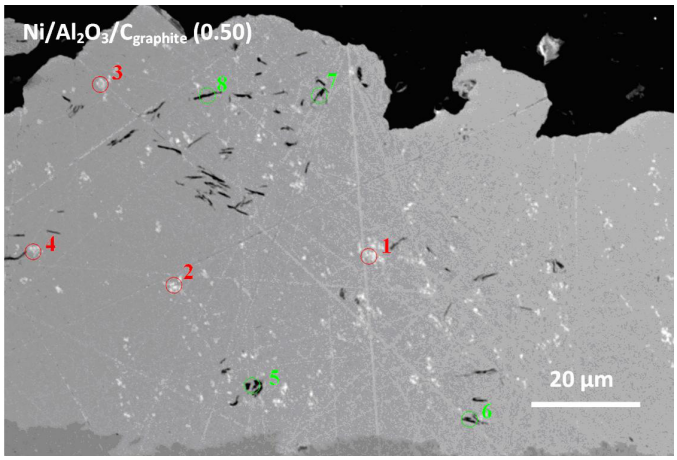

Fig. 7. Cross-section of $Ni/Al_2O_3/C_{graphite}$ (0.50) composite layer with marked areas of chemical composition analysis

TABLE 3

The results of point analysis of chemical composition of $Ni/Al_2O_3/C_{graphite}$ (0.25) composite layer

point 1		point 2		point 3		point 4	
elem.	at. %	elem.	at. %	elem.	at. %	elem.	at. %
C	3.94	C	3.96	C	4.54	C	4.48
O	8.22	O	12.48	O	7.77	O	13.24
Al	4.95	Al	7.93	A	4.86	Al	8.42
Ni	82.90	Ni	75.63	Ni	82.83	Ni	73.85
point 5		point 6		point 7		point 8	
elem.	at. %	elem.	at. %	elem.	at. %	elem.	at. %
C	91.18	C	81.04	C	87.19	C	47.97
O	—	O	—	O	—	O	1.54
Ni	8.82	Ni	18.96	Ni	12.81	Ni	50.49

TABLE 4

The results of point analysis of chemical composition of $Ni/Al_2O_3/C_{graphite}$ (0.50) composite layer

point 1		point 2		point 3		point 4	
elem.	at. %	elem.	at. %	elem.	at. %	elem.	at. %
C	3.53	C	4.15	C	3.84	C	4.35
O	24.60	O	16.79	O	18.66	O	10.93
Al	15.79	Al	10.85	Al	12.11	Al	7.00
Ni	56.07	Ni	68.21	Ni	65.39	Ni	77.72
point 5		point 6		point 7		point 8	
elem.	at. %	elem.	at. %	elem.	at. %	elem.	at. %
C	65.66	C	40.28	C	66.12	C	69.88
O	1.66	O	1.69	O	2.09	O	–
Ni	32.68	Ni	58.04	Ni	31.78	Ni	30.12

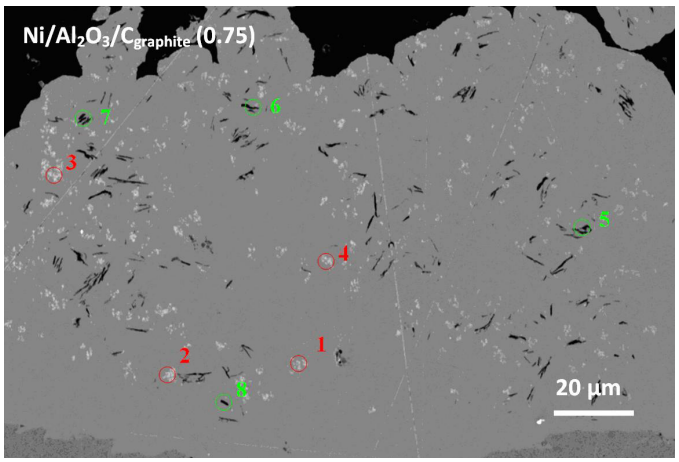

Fig. 8. Cross-section of Ni/Al_2O_3/Cgraphite (0.75) composite layer with marked areas of chemical composition analysis

TABLE 5

The results of point analysis of chemical composition of Ni/Al_2O_3/C_{grafit} (0.75) composite layer

point 1		point 2		point 3		point 4	
elem.	**at. %**	**elem.**	**at. %**	**elem.**	**at. %**	**elem.**	**at. %**
C	3.95	C	4.33	C	4.30	C	4.66
O	11.90	O	10.09	O	14.35	O	10.20
Al	7.73	Al	6.52	Al	9.29	Al	6.08
Ni	76.42	Ni	79.07	Ni	72.06	Ni	79.07
point 5		**point 6**		**point 7**		**point 8**	
elem.	**at. %**	**elem.**	**at. %**	**elem.**	**at. %**	**elem.**	**at. %**
C	49.26	C	71.59	C	61.90	C	92.21
Ni	50.74	Ni	28.41	Ni	38.10	Ni	7.79

materials by incorporation of dispersion phases influences on improvement of corrosion resistance [16,18]. Figure 10 presents the corrosion damage of examined layers in 0.5 M NaCl environment. In all cases, the corrosion damages are local and take the form of pitting corrosion, what is characteristic for nickel layers [19].

The influence of the type of dispersion phase on the corrosion resistance of nickel matrix composite layers in the environment of 0.5 M NaCl solution was investigated in work [7]. Corrosion parameters of Ni/Al_2O_3 and Ni/$C_{graphite}$ composite layers as well as the Ni/Al_2O_3/$C_{graphite}$ hybrid composite layer produced in baths containing 2 g/dm^3 of each of dispersion phases determined in work [7] are presented in Table 7.

The graphite as one of incorporated dispersion phases increases the degree of surface development of layers resulting in decrease of corrosion resistance of composite layers.

The measurements results of layers microhardness by Knoop method have been shown on Figure 11.

Incorporation of dispersion phases particles into nickel matrix increases the hardness of the layer material. The highest hardness equal to 636 HK0.01 (~600 HV) is exhibited by the hybrid composite layer produced in the bath with the highest amount of dispersion phases particles. The increase of hardness of hybrid composite layers can be explained by existence of two mechanisms of strengthening: the grain refinement strengthening

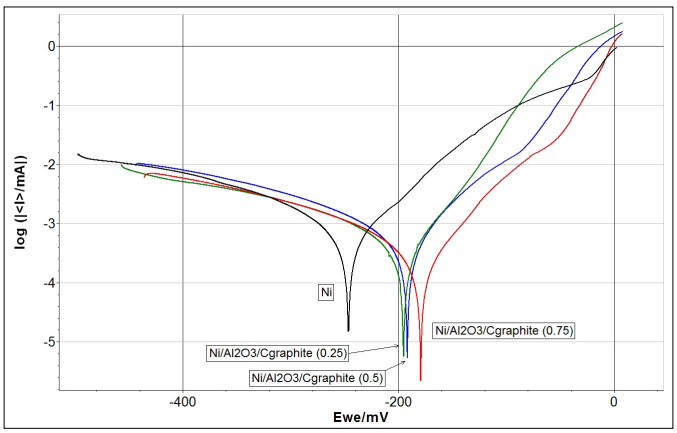

Fig. 9. Potenciodynamic curves of deposited layers

TABLE 6

Corrosion parameters of produced layers in 0.5 M NaCl environment

Layer	E_{cor} [mV]	I_{cor} [µA/cm^2]
Ni	–246	0.367
Ni/Al_2O_3/$C_{graphite}$ (0.25)	–195	0.224
Ni/Al_2O_3/$C_{graphite}$ (0.50)	–191	0.254
Ni/Al_2O_3/$C_{graphite}$ (0.75)	–179	0.123

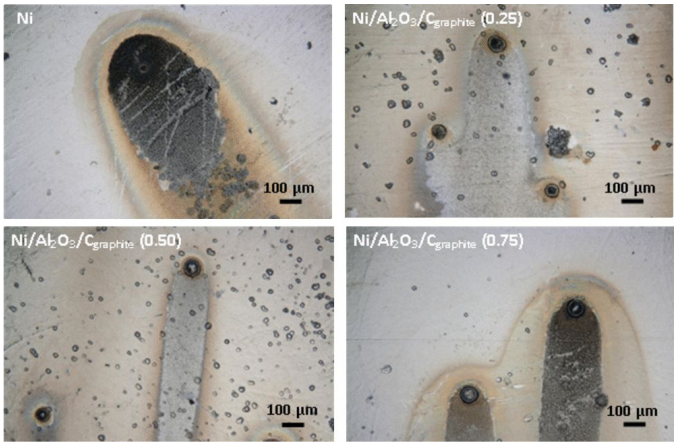

Fig. 10. Image of the surface of produced layers after corrosion tests in 0.5 M NaCl environment

TABLE 7

Corrosion parameters of composite layers in 0,5 M NaCl environment [7]

Layer	E_{cor} [mV]	I_{cor} [µA/cm^2]
Ni/Al_2O_3	–134	0.022
Ni/$C_{graphite}$	–355	2.837
Ni/Al_2O_3/$C_{graphite}$	–243	0.231

and dispersion strengthening [20,21]. As a result of incorporation of dispersion phase particles into nickel matrix, the structure of layer material is refining, what leads to the occurrence in the material more grain boundaries, which are barriers to the dislocation mobility, and this leads to the strengthening of the

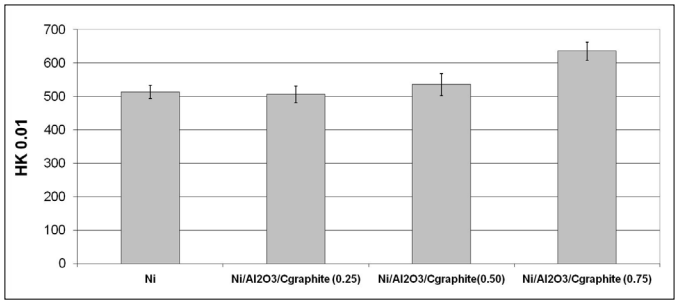

Fig. 11. Microhardness of deposited layers

material. In the case of dispersion strengthening, the dislocation mobility is blocked by dispersion phase particles embedded into matrix material [15,21]. The type and content of incorporated dispersion phase into nickel matrix has an impact to hardness of composite material. Incorporation of Al_2O_3 particles into nickel matrix increases the hardness of Ni/Al_2O_3 composite layers, which is about 500-700 HV, depending on the electrocrystallization parameters and content of particles in the bath [22-25]. In the case of Ni/$C_{graphite}$ composite layers, incorporation of graphite particles into nickel matrix decreases the hardness of layers even up to 30% [26,27].

The investigations of mechanical properties by DSI method included the determination of loading/unloading curves as F(h) function of the tested layers. Figure 12 shows the determined curves of dependence of penetration depth (h) of the indenter as the function of the given load (F) for Ni and Ni/Al_2O_3/$C_{graphite}$ (0.75) layers.

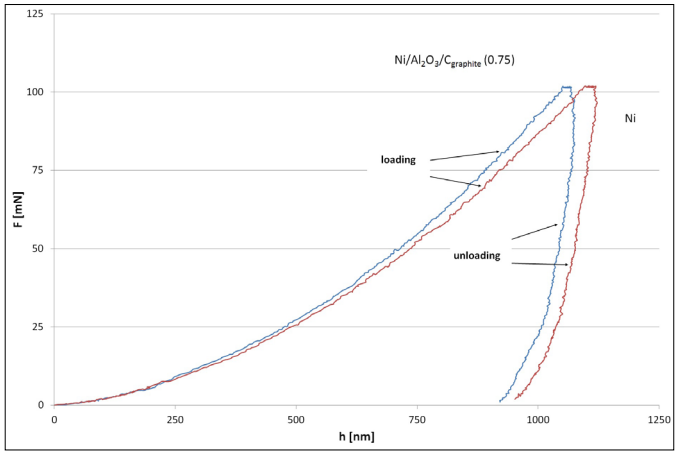

Fig. 12. Curves of loading/unloading for Ni and Ni/Al_2O_3/$C_{graphite}$ (0.75) layers

Based on the ability of the indenter penetration in material of tested layers, the modulus of elasticity E_{IT}, Indention hardness H_{IT} and Martens hardness H_M were determined. The results of the determined DSI parameters of Ni and Ni/Al_2O_3/$C_{graphite}$ (0.75) layer materials are presented in Table 8.

The hybrid composite layer are characterized by lower susceptibility for the deformation than the nickel layer – its curve of loading/unloading has narrower hysteresis loop and is shifted towards to the axis of abscissa. It is confirmed by the

TABLE 8

Results of hardness and modulus of elasticy of Ni and Ni/Al_2O_3/$C_{graphite}$ layers

Layer	H_{IT} [MPa]	H_M [MPa]	E_{IT} [GPa]
Ni	3709	3076	227
Ni/Al_2O_3/$C_{graphite}$ (0.75)	4088	3399	253

results of hardness and modulus of elasticity, which are higher for hybrid composite layer, due to finer grain size and effects of dispersion strengthening. The measurement results of wear resistance by ball-on-disc method are shown in Figure 13. Figure 14 presents the images of layers surface after the tests of the wear resistance.

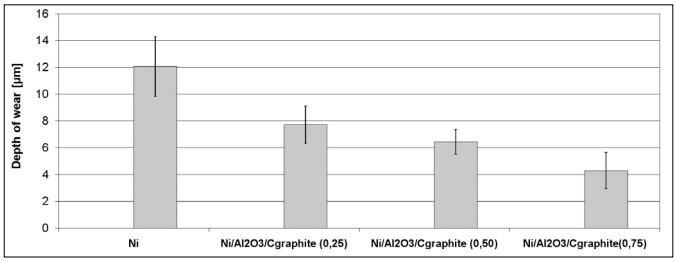

Fig. 13. Measurement results of the wear resistance of produced layers

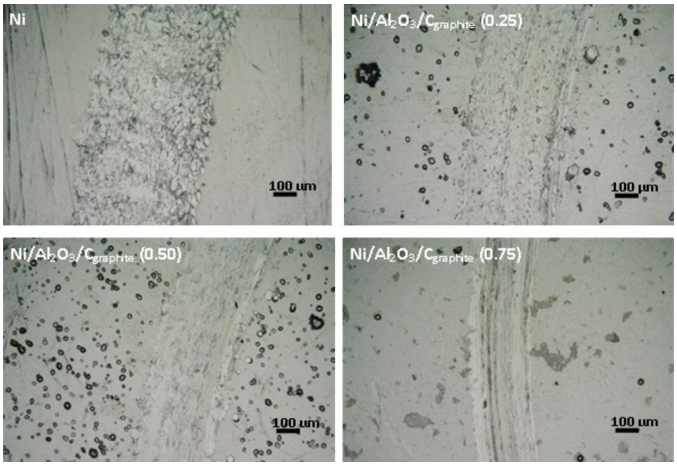

Fig. 14. Image of the surface of produced layers after the wear resistance tests

The incorporation of dispersion phase particles into nickel matrix increases the wear resistance, what correlates with the hardness results. The highest wear resistance, almost three times higher in relation to the nickel layer, is exhibited by the hybrid composite layer produced from the bath with the highest content of both dispersion phases. Improvement of the wear resistance of hybrid composite layers is caused by the structure refining and dispersion strengthening (Orowan mechanism) [15,20]. The highest impacts for the improvement of wear resistance have embedded flakes of graphite into layer material, due to its self-lubricating properties. Layered structures of the graphite and easiness of bond-breaking among the adjacent graphene

planes favor gliding between the layers. During the dry friction a self-lubricating film is formed in the contact zone, what results in decreasing of the friction coefficient of the layer whereby to the lower material wear [26,28]. The results obtained in our investigations are compatible with other authors results, mainly, incorporation of graphite particles into nickel matrix increases the wear resistance of $Ni/C_{graphite}$ composite layers [26,27], and incorporation of Al_2O_3 particles also increases the wear resistance of composite layers but to a lesser extent [3,23,24,29]. Wan-chang Sun et al. [28] observed a relationship between concentration of graphite in the bath (from 0 to 2.5 g/L) and wear resistance of $Ni\text{-}Al_2O_3$/graphite composite layers. With the increasing content of the graphite particles in the bath with a constant content of Al_2O_3 particles the wear loss decreases, which was explained by forming the transfer film by graphite which reduce friction coefficient of layers. Also in work [27], where $Ni/C_{graphite}$ composite layers were investigated authors obtained three times higher increase of wear resistance compared to Ni layer.

4. Conclusions

Composite layers consisting of the nanocrystalline nickel matrix and two types of incorporated dispersion phases in the form of Al_2O_3 and graphite powder particles were produced by electrocrystallization method. Produced layers are characterized by compact structure and good adhesion to the substrate. The crystalline structure of layer material has been refined as a result of embedding a dispersion phase particle. The hybrid composite layers are characterized by a higher degree of surface development compared to the nickel layer. Furthermore, the incorporation of Al_2O_3 and graphite particles increases the corrosion resistance, hardness and wear resistance. The hybrid composite layer produced in the bath with the highest content of both dispersion phases (0.75 g/dm^3) are characterized by the best mechanical and corrosion properties.

REFERENCES

[1] S. Arshali, M. Manoj, D. Saurabh, K. Sasi, Mater. Today-Proc. **2**, 3042-3048 (2015).

[2] S. Özkana, G. Hapçıa, G. Orhana, K. Kazmanlıb, Surf. Coat. Tech. **232**, 734-741 (2013).

[3] T. Borkar, S.P. Harimkar, Surf. Coat. Tech. **205**, 4124-4134 (2011).

[4] M. Surender, B. Basu, R. Balasubramaniam, Tribol. Int. **37**, 743-749 (2004).

[5] P. Baghery, M. Farzam, A.B. Mousavi, M. Hosseini, Surf. Coat. Tech. **204** (23), 3804-3810 (2010).

[6] G. Cieślak, M. Trzaska, Pol. J. Chem. Technol. **20** (1), 29-34 (2018).

[7] W. Bartoszek, G. Cieślak, K. Skroban, A. Mazurek, M. Trzaska, Ochrona przed Korozją **61** (2), 36-39 (2018).

[8] N.P. Wasekar, P. Haridoss, S.K. Seshadri, G. Sundararajan, Surf. Coat. Tech. **291**, 130-140 (2016).

[9] A.C. Ferrari, J.C. Meyer, V. Scardaci, C. Casiraghi, M. Lazzeri, F. Mauri, S. Piscanec, D. Jiang, K.S. Novoselov, S. Roth, A.K. Geim, Phys. Rev. Lett. **97**, 187401 (2006).

[10] I. Childres, L.A. Jauregui, W. Park, H. Cao, Y.P. Chen, Raman spectroscopy of graphene and related materials, in: J.I. Jang (Ed.), New Developments in Photon and Materials Research, Nova Science Publishers, 2013

[11] S. Reich, C. Thomsen, Phil. Trans. R. Soc. Lond. A **362**, 2271-2288 (2004).

[12] https://www.thermofisher.com/content/dam/tfs/ATG/CAD/CAD%20Documents/Application%20&%20Technical%20Notes/Molecular%20Spectroscopy/Raman/Raman%20Instruments/AN52252_E%201111%20LayerThkns_H_1.pdf, accessed: 20.07.2018

[13] https://assets.thermofisher.com/TFS-Assets/CAD/Application-Notes/D19504~.pdf, accessed: 20.07.2018

[14] M. A. Karimi, F. Banifatemeh, M. Ranjbar, J. Mater. Sci.-Mater. El. **28**, 1844-1851 (2017).

[15] M.R. Vaezi, S.K. Sadrnezhaad, L. Nikzad, Colloid Surface A. **315**, 176-182 (2007).

[16] S. Dehgahi, R. Amini, M. Alizadeh, Surf. Coat. Tech. **304**, 502-511 (2016).

[17] Q. Fenga, T. Lia, H. Tenga, X. Zhanga, Y. Zhanga, C. Liub, J. Jina, Surf. Coat. Tech. **202** (17), 4137-4144 (2008).

[18] S. Dehgahi, R. Amini, M. Alizadeh, J. Alloy Compd. **692**, 622-628 (2017).

[19] A. Mazurek, G. Cieślak, M. Trzaska, Prace Szkoły Inżynierii Materiałowej XLIV, Akapit, Kraków (2016).

[20] F. Hou, W. Wang, H. Guo, Appl. Surf. Sci. **252** (10), 3812-3817 (2006).

[21] Y. Zhou, H. Zhang, B. Qian, Appl. Surf. Sci. **253** (20), 8335-8339 (2007).

[22] E. Beltowska-Lehman, A. Góral, P. Indyka, Arch. Metall. Mater. **56** (4), 919-931 (2011).

[23] H. Gül, F. Kılıc, S. Aslan, A. Alp, H. Akbulut, Wear **267**, 976-990 (2009).

[24] L. Du, B. Xu, S. Dong, H. Yang, Y. Wu, Surf. Coat. Tech. **192**, 311-316 (2005).

[25] R.K. Saha, T.I. Khan, Surf. Coat. Tech. **205**, 890-895 (2010).

[26] H. Zhao, L. Liu, W. Hu, B. Shen, Mater. Design. **28** (4), 1374-1378 (2007).

[27] M. Trzaska, M. Gostomska, Kompozyty **9**, 1, 84-88 (2009).

[28] W. Sun, P. Zhang, K. Zhao, M. Tian, Y. Wang, Wear. 342-343, 172-180 (2015).

[29] L. Du, B. Xu, S. Dong, H. Yang, W. Tu, Wear **257**, 1058-1063 (2004).